Elastin receptor (S-gal) occupancy by elastin peptides modulates T-cell response during murine emphysema

Aïda Meghraoui-Kheddar, Alexandre Pierre, Mehdi Sellami, Sandra Audonnet, Flora Lemaire, Richard Le Naour

Elastin receptor (S-gal) occupancy by elastin peptides modulates T cell response during murine emphysema

Aïda Meghraoui-Kheddar,[1] Alexandre Pierre,[1] Mehdi Sellami,[1] Sandra Audonnet,[2] Flora Lemaire,[1] Richard Le Naour[1]

Author contributions: A.M-K. and R.L.N. have 1) contributed to conception and design, 2) analyzed and interpreted data, 3) drafted the article and 4) approved the final version to be published. A.M-K., A.P. M.S. and F.L. have performed experiments. S.D. has 1) analyzed flow cytometry data and 2) critically revised the manuscript. All authors have approved the manuscript submission.

Affiliations: [1]EA4683, SFR CAP-Santé, Université de Reims Champagne-Ardenne, Reims, France**.** [2]Plateau technique de cytométrie en flux, Plateforme Santé, URCA, Reims, France.

Running head: Elastin-dependent T cell response during murine emphysema

Address for reprint requests and other correspondence: Richard Le Naour, EA4683 "Immunité Adaptative et Fonctionnalité des Barrières Biologiques", UFR de Pharmacie, 1 rue du Maréchal Juin 51096 Reims cedex, France. E-mail: richard.lenaour@univ-reims.fr

Abstract

Chronic obstructive pulmonary disease and emphysema are associated with increased elastin peptides (EP) production due to excessive breakdown of lung connective tissue. We recently reported that exposure of mice to EP elicited hallmark features of emphysema. EP effects are largely mediated through a receptor complex which includes the elastin-binding protein S-gal. In previous studies, we established a correlation between cytokine production and S-gal protein expression in EP treated immune cells. In this study, we investigated the S-gal-dependent EP effects on T helper (Th) and T cytotoxic (Tc) responses during murine EP-triggered pulmonary inflammation. C57BL/6J mice were endotracheally instilled with the VGVAPG elastin peptide and 21 days after treatment, local and systemic T lymphocyte phenotypes were analyzed at cytokine and transcription factor expression levels by multicolor flow cytometry. Exposure of mice to the VGVAPG peptide resulted in a significant increase in the proportion of the $CD4^+$ and $CD8^+$ T cells expressing the cytokines IFN-γ or IL-17a and the transcription factors Tbet or RORγt without effects on IL-4 and Gata3 expression. These effects were maximized when each T cell sub-population was challenged *ex vivo* with EP and they were inhibited *in vivo* when an analogous peptide antagonizing the EP/S-gal interactions was instilled together with the VGVAPG peptide. This study demonstrates that during murine emphysema, EP/S-gal interactions contribute to a Th-1 and Th-17 pro-inflammatory T cell response combined with a Tc-1 response. Our study also highlights the S-gal receptor as a putative pharmacological target to modulate such an immune response.

Keywords: murine model, VGVAPG, T lymphocytes, IFN-γ, IL-17

INTRODUCTION

Chronic obstructive pulmonary disease (COPD), one of the leading health issues worldwide, is characterized by a progressive airflow limitation that is associated with a chronic inflammatory response in the airways. This persistent inflammatory state may induce pulmonary emphysema and small airway fibrosis (41). Whereas neutrophils and macrophages have been described as key effector cells involved in COPD pathogenesis, recent studies have emphasized on the role of other immune cells such as NK cells (40), NKT cells (11) and T lymphocytes in the pulmonary inflammation process and emphysema development. Focusing on T cells, numerous studies reported the presence of $CD4^+$ and $CD8^+$ T lymphocytes in both airways and parenchyma during COPD (14, 15, 30) and the relationship between increase in these cell populations and a greater disease severity (7, 8, 18). Increase of T helper (Th)-1 (17, 24), Th-2 (3, 31) or Th-17 (8, 36) cytokine expression was described in peripheral blood, broncho-alveolar lavages (BAL) or intraepithelial COPD-associated T cells. It is now accepted that emphysema is partly driven by pathogenic T cells inducing inflammatory damages, but the critical role of $CD4^+$ Th cells versus $CD8^+$ T cytotoxic (Tc) cells in emphysema remains controversial and their orientation in COPD is still unclear.

In COPD patients, a massive proteases production by lung-infiltrating inflammatory cells was described (26), supporting the protease/antiprotease imbalance theory during the pathology (27). Some of these proteases promote degradation of pulmonary elastin (23). Accordingly, an increased secretion of desmosine, a specific marker for elastin degradation (13), and elevated levels of soluble elastin peptides (EP) in various biological fluids of COPD patients reflect massive pulmonary elastin breakdown (9, 32). In emphysematous animal models, circulating EP are associated with the lysis of nearly 60% of pulmonary elastic fibers (13). EP produced in significant amounts during proteolytic degradation of lung share miscellaneous biological activities, predominantly chemotactic activities (35) and protease

release (9) that are directly involved in propagation and maintenance of inflammation associated with emphysema.

EP exhibit a wide range of biological activities (9, 12, 35) that can be attributed in their whole to the VGVAPG hexa-peptide, a peptide sequence repeated several times in the elastin monomer and the major ligand for the high affinity binding site of a receptor complex that includes a 67-kDa elastin-binding protein which is an enzymatically inactive spliced variant of β-galactosidase called Spliced-galactosidase (S-gal) (16). In immune cells, we previously demonstrated that EP/S-gal interactions modulate expression of pro-inflammatory cytokines in monocytes (1) and promote a pro-inflammatory Th-1 response in stimulated human peripheral blood lymphocytes (5). Moreover, the immunogenicity of EP was investigated during COPD and anti-elastin B-cell response was reported (22). The emergence of auto-reactive T cell clones was also described during emphysema (44) and recently reported in COPD patients (4). Interestingly, we defined in our last works a correlation between EP/S-gal interactions and alteration of neutrophil functions in COPD patients (9) or induction of emphysema-like phenotype in EP-treated mice (34).

Since EP/S-gal interactions regulate T cell response and promote development of emphysema process, we here hypothesized that such an interaction may be also involved in the emphysema-associated $CD4^+$ and $CD8^+$ T cell response. In this study, we demonstrated that in mice Th-1, Th-17 and Tc-1 pro-inflammatory responses observed during EP-induced emphysema could be modulated using S-gal-specific antagonist peptides.

MATERIALS AND METHODS

Animal procedure. Six-week old C57BL/6J female mice purchased from Harlan Sprague Dawley (Harlan Laboratories, Gannat, France) were housed in an animal facility that was maintained at 22-26°C with 40-69% humidity and a 12-h light/dark cycle. Animals were fed with a commercial diet and received water *ad libitum*. Animals were humanely cared for, and all animal experiments were approved by the University of Reims Champagne-Ardenne Institutional Animal Care and Use Committee and were carried out in accordance with institutional guidelines and regulations. After appropriate sedation, mouse lungs were endotracheally instilled with either PBS, or one unit (7.4 µg) porcine pancreatic elastase (PPE) (Sigma-Aldrich, Saint-Quentin Fallavier, France), or 10 µg VGVAPG (Genepep SA, Saint Jean de Védas, France), or 10 µg PGAIP (Genepep SA) via a 22-gauge i.v. catheter in a total volume of 50 µl PBS as previously described (34). In some experiments, we co-administrated the analogous antagonist peptide PGAIP to VGVAPG-recipient mice or to PPE-recipient mice to evaluate the capacity of this peptide to neutralize the VGVAPG- or PPE-induced T cell response. In these experiments, animals received 50 µl of PBS containing a single mixture of VGVAPG (10 µg) and PGAIP (10 µg), or PPE (7.4 µg) and PGAIP (10 µg) at time 0 and were sacrificed on the 21st day. Animals were sacrificed on days 2 and 21. At day 2, bronchoalveolar lavage fluids (BALF) were recovered to analyse cell profiles. At day 21, BALF were also recovered to determine desmosine concentrations. At the same time, lungs, mediastinal lymph nodes (mLN) and spleens were recovered to investigate the profile of the tissue specific $CD4^+$ and $CD8^+$ T cells. Peripheral blood of mice was collected by cardiac puncture and *sera* stored at -80°C for further measurement of circulating desmosine concentration. Then, the pulmonary and systemic circulation of euthanized mice was perfused with sterile PBS to remove the intravascular pool of cells. Spleen was dissected away from the surrounding tissue, and mLN were then collected. Lungs were carefully separated from

thymic, cardiovascular remnants and main bronchi and trachea. Lungs from appropriate mice were also inflated, removed and embedded in paraffin to allow morphological and elastin/collagen network analysis.

Synthesis, purification and characterization of EP. Synthesis of the elastin peptides used in this study (VGVAPG and PGAIPG) was performed by Genepep (Genepep SA, Saint Jean de Védas, France). Crude peptides were purified by RP-HPLC on a semi-preparative C18-bonded silica column using a Shimadzu SPD 10A UV/VIS detector, with detection at 210 and 254 nm. The column was perfused at a flow rate of 3 ml/min with solvent A (10%, v/v, water in 0.1% aqueous TFA), and a linear gradient from 10 to 90% of solvent B (80%, v/v, acetonitrile in 0.1% aqueous TFA) over 40 min was adopted for peptide elution. Analytical purity and retention time of each peptide were determined using HPLC conditions in the above solvent system (solvents A and B). All analogous peptides showed >98% purity when monitored at 215 nm. Homogeneous fractions, as established using analytical HPLC, were pooled and lyophilized. Peptides molecular weights were determined by ESI mass spectrometry. ESI-MS analysis was made in positive ion mode. The sample was dissolved in a mixture of water and methanol (50/50) and injected directly into the electrospray source, using a syringe pump, which maintains constant flow at 5 µl/min. The temperature of the capillary was set at 220 °C. All peptides used in this study were solubilized or diluted in PBS.

Broncho-alveolar lavage. The trachea was inserted with a 22-gauge i.v. catheter, and the whole lungs were washed three times with 1 ml PBS. BALF was centrifuged at 300 x *g* for 10 min at +4°C, and the supernatant was collected and stored at -80°C until required. Cell pellet was resuspended in 1 ml of PBS, and cell count was performed. Cell viability was more than 95% as determined by trypan blue exclusion. Aliquots of cells were then stained with fluorescent mAb specific for leucocytes (CD45, BD Biosciences, Le pont de Claix, France), neutrophils (Ly6G, BD Biosciences), macrophages (Mac3, BD Biosciences), B lymphocytes

(CD19, BD Biosciences), and T lymphocyte sub-populations (CD3, CD4 and CD8, BD Biosciences). Flow cytometry analysis was performed and absolute number in cell populations was calculated.

Lung tissue preparation. The lungs were inflated for 10 min at a constant pressure of 25 cm H_2O in the presence of 10% neutral buffered formalin solution (Sigma-Aldrich) and then removed. Formalin inflated lungs were fixed in 4% PFA for 24 h at room temperature before embedding in paraffin. Then, transverse 3-µm or 20-µm sections of lung were cut for morphological or collagen and elastin network analysis, respectively.

Lung, mLN and spleen cell preparation and culture. Lungs were thoroughly chopped in using iridectomy scissors and incubated in digestion medium (Macs Miltenyi Biotec, Paris, France) for 30 min at 37°C under permanent agitation of 60 rpm. Lung fragments were resuspended in fresh digestion medium, passed through a successive 70-µm and 40-µm cell strainers and centrifuged. Red blood cells were then lysed using RBC Lysis Solution (Miltenyi Biotec) and washed with X-VIVO 15 serum free medium (Lonza, Verviers, Belgium). mLN were passed through a 70-µm cell strainer, using a 1 mL syringe plunger, and washed in X-VIVO 15 serum free medium (Lonza). Spleens were also passed through a successive 70-µm and 40-µm cell strainers, using a 5 mL syringe plunger-and washed twice. The $CD45^+$ leucocytes were isolated from lung single-cell suspensions by immuno-magnetic positive selection using mouse anti-CD45 microbeads according to the manufacturer's instructions (Miltenyi Biotec). Cell purity and viability were respectively over 98% and 90% as determined by flow cytometry analysis. Phenotypic analysis of mLN single-cell suspensions by flow cytometry revealed over 90% of $CD45^+$ cells, so no sorting were performed. $CD4^+$ and $CD8^+$ T cells were separately isolated from spleen single-cell suspensions by immuno-magnetic depletion using mouse $CD4^+$ Isolation Kit II and $CD8^+$ T cell Isolation Kit respectively, according to the manufacturer's instructions (Miltenyi Biotec).

Cell purity and viability were respectively over 90% and 95% as determined by flow cytometry analysis. $CD45^+$ leucocytes either from lungs or mLN were cultured in 96-well culture plates (4 x 10^6 cells/ mL) and incubated with Dynabeads mouse T-activator beads (Invitrogen, Illkirch, France) coated with antibodies against CD3 and CD28. Isolated $CD4^+$ and $CD8^+$ splenic T cells were cultured in 48-well culture plates (2 x 10^6 cells/mL) and incubated with Dynabeads mouse T-activator beads (Invitrogen) in the presence or not of the VGVAPG peptide (20 µg/ mL) or an elastin peptide mixture (EPM) obtained by the digestion of lung elastic fibers with neutrophil elastases (Elastin Products Co., Owensville, MO, USA). After 48 h incubation, stimulated cells from lungs, mLN and spleens were stained and analyzed by flow cytometry.

Morphological analysis. Serial mid-sagittal sections (3-µm thick) stained with Hematoxylin Phloxin Safran were used for morphological analysis. Ten randomly selected (100x) fields per slide were photographed using the ZEN imaging software (Carl Zeiss SAS, Marly-Le-Roi, France). The images were analyzed using the Image J software (NIH, Bethesda, MD, USA). From each fields ten areas of interest, free of airways and muscular blood vessels, were picked for measurement of the number of intersections of virtual lines of known length, with alveolar septa. An increase in the average distance between intercepts (mean linear intercept) indicates enlarged airspaces.

Collagen and elastin network acquisition and quantification. Serial unstained mid-sagittal sections (20-µm thick) were used for the simultaneous visualization of collagen and elastin in lung tissue section based on collection of second-harmonic generation (SHG) and two photons excited fluorescence (2PEF) signals, respectively, as described previously (34). Volume ratio of elastin and collagen structures were computed in term of the voxel volumes as previously described (34). The volume fraction estimation of elastin and collagen structures was performed after 3D reconstruction images from 2PEF/SHG data sets

processing with the Imaris software (Bitplane AG, Zurich, Switzerland). The ratio index, calculated in order to evaluate the elastin destruction in lung tissue, is defined as follow: Ratio index = (*E*v-*C*v)/(*E*v+*C*v), where *E*v and *C*v represent elastin and collagen voxel volumes, respectively. This ratio index approaches maximum value of +1 when only elastin is present, and this ratio index approaches minimum value of -1 when only collagen is present. This ratio index therefore provides an estimation of the extent of ECM remodeling in terms of collagen and elastin voxel volumes in the lung tissues undergoing emphysematous destruction.

Quantification of cytokine secretion. Determination of IFN-γ, IL-17a and IL-4 concentrations in the cell culture supernatants of stimulated $CD4^+$ and $CD8^+$ splenic T cells was performed using commercially available Cytometric Bead Array (CBA) Flex Set technology (BD Biosciences) according to the manufacturer's instructions. CBA Flex Set capture bead is a single bead population with distinct fluorescence intensity and is coated with a capture antibody specific for a soluble protein. Preparation of samples was done according to the manufacturer's instructions. Briefly, serial dilutions (1/2, v/v) of the standard preparations were prepared whereas culture supernatants were used undiluted. Then, 50 µL of mixed capture beads were added to each sample. After 1 h incubation period at room temperature, 50 µL of PE detection reagent was added and samples were incubated for another 1 h at room temperature. Samples were then washed twice at 400 x *g* for 10 min and 150 µL wash buffer was added. Flow cytometry analysis was performed using BD LSRFortessa cell analyzer and CBA analysis FCAP software (BD Biosciences). A total of 700 events were acquired per analyte. The minimum detection level for each cytokine was 0.5 pg/mL, 0.95 pg/mL and 0.3 pg/mL for IFN-γ, IL-17a and IL-4, respectively.

Desmosine quantification. Determination of desmosine concentrations in BAL fluids and *sera* was performed in triplicate using a commercially available ELISA kit (Cusabio Biotech product, Interchim, Montluçon, France) according to manufacturer's instructions. The

sensitivity of ELISA kit was 0.78 pg/ml.

Flow cytometry analysis. Analysis of the surface antigens, intracellular cytokine and intra-nuclear transcription factor expressed on stimulated $CD45^+$ leucocytes or sorted lymphocytes isolated from BALF, lung, mLN or spleen were performed using antibodies listed in Table 1 and at a target concentration determined from dose/effect specific curves. Cells were treated with Cytofix / CytoPerm or Transcriptional Factor buffer set (BD Biosciences) before incubation with intracytoplasmic antibodies or intranuclear antibodies respectively. Whatever the experimental conditions used, incubation with antibodies was performed during 20 min at +4°C and in the dark. Following two successive centrifugations (300 x g, 10 min), pellets of stained cells were resuspended in 300 µL PBS containing 1% PFA, and stored in the dark at +4°C until analysis (at the latest 72 h after staining). In all protocols, fluorescence emission was assessed by flow cytometry using BD LSRFortessa (BD Biosciences) cell analyzer and BD Diva (BD Biosciences) and FlowJo (FlowJo, Ashland, USA) softwares. As compensation controls, OneComp eBeads were used (Biosciences Company, Paris, France) and isotype controls of each monoclonal antibody and fluorescence minus one tubes were used to assess negative population.

Statistical analysis. Data are presented as means±SEM. Difference among groups was analyzed using one-way ANOVA followed by the Bonferroni *post hoc* test. For all analyses, a p value < 0.05 was considered statistically significant. All statistical analyses were performed using GraphPad Prism (GraphPad software San Diego, CA, USA).

RESULTS

The VGVAPG peptide-induced emphysema is associated with an early CD4$^+$ and CD8$^+$ T lymphocyte infiltrate in BALF. We previously demonstrated that mice instilled with VGVAPG, an elastin hexa-peptide, exhibited lung accumulation of inflammatory cells (macrophages and neutrophils), high concentration of desmosine in BALF and emphysematous structural changes similar to those observed following endotracheal administration of PPE (34). Here, we examine the lymphocyte cell infiltration in the BALF of EP-exposed mice. Two days after exposure to one single dose of the VGVAPG peptide (10µg) delivered into the trachea of WT C57BL/6J mice, flow cytometry analysis of BALF was performed and absolute number of cells was calculated. As expected, total cells in the BALF of VGVAPG-treated mice were found to be at least threefold higher than BALF total cells of PBS-treated group, with a majority of macrophages and neutrophils (Fig. 1*A*). A significant increase of infiltrating T lymphocytes through CD4$^+$ and CD8$^+$ T cell subpopulations was also observed in VGVAPG-instilled mice when compared to control group. This result was also obtained following administration of a single dose of PPE (7.4µg). VGVAPG-dependent cellular accumulation in BALF was associated at day 21 to histological characteristics of emphysema. A breakdown of elastin and collagen fibers was observed in lung tissue (Fig. 1*B*) and confirmed by decrease of the ratio index that provides a quantification of the extent of extracellular matrix remodelling in terms of elastin and collagen structures (Fig. 1*C*). Extracellular matrix remodeling after 21 days was accompanied by significant airspace enlargement (Fig. 1*D*) as revealed by increase of mean linear intercept values representative of the alveolar space size (Fig. 1*E*). The elastin fibers breakdown related to VGVAPG administration was also confirmed at day 21 by the increase of desmosine concentration in BAL fluids and *sera* compared to control condition. The desmosine levels were similar between VGVAPG and PPE groups (Fig. 1*F*).

The VGVAPG peptide induces a local and systemic Th-1/Th-17 and Tc-1 response during murine emphysema. We next examined at day 21 the levels of type 1 (IFN-γ), type 2 (IL-4) and type 17 (IL-17a) cytokines expressed by $CD4^+$ and $CD8^+$ T lymphocytes either locally (lung tissue and mLN) or at systemic level (spleen). Flow cytometry analysis of anti-CD3/CD28-activated $CD4^+CD25^+$ T cells showed that, in all three tissue types, expression of intracellular IFN-γ or IL-17a was significantly higher in VGVAPG-treated mice than in PBS-treated mice, whereas intracellular IL-4 expression was not altered by VGVAPG treatment (Fig. 2*A*). Interestingly, the proportion of $CD4^+CD25^+$ T cells expressing IFN-γ was constantly greater than the proportion of T cells expressing IL-17a in the two mice groups. Th-1 and Th-17 differentiation are driven by the transcription factors T-bet (39) and RORγt (20), respectively. We found that expression of the transcription factors T-bet or RORγt by activated $CD4^+CD25^+$ T cells was stronger in lung tissue, mLN and spleen after VGVAPG treatment (Fig. 2*B*). As expected, exposure to VGVAPG did not affect expression of the type-2 specific transcription factor GATA3 by activated $CD4^+CD25^+$ T cells (Fig. 2*B*). A significant increase of IFN-γ and T-bet transcription factor was also observed in activated $CD8^+CD25^+$ T cells isolated from lung, mLN or spleen of VGVAPG instilled mice (Fig. 3*A* and 3*B*). In contrast, exposure to VGVAPG did not impact the expression of neither IL-17a and IL-4 intracellular cytokines nor RORγt and GATA3 transcription factors in these cells (Fig. 3*A* and 3*B*). Similar results were obtained after endotracheal administration of PPE (Fig. 2 and Fig. 3). Consistent with both intracellular and intra-nuclear analysis of activated splenic T cells, CBA assay showed an important IFN-γ and, to a lesser extent, IL-17a cytokine production by stimulated $CD4^+$ splenic T cells isolated from VGVAPG- or PPE-treated groups, whereas no difference was observed in $CD4^+$ T cell-derived IL-4 production whatever the group analysed (Fig. 4*A*). Likewise, a massive production of IFN-γ was detected after

anti-CD3/CD28 stimulation of splenic $CD8^+$ T cells isolated from either VGVAPG or PPE emphysematous mice (Fig. 4*B*).

Treg cell proportion is not altered in lung, mLN and spleen of VGVAPG-instilled mice. The typical balance between Th-17 and Treg, and to a lesser extent between Th-1 and Treg (42), led us to investigate the consequences of VGVAPG endotracheal instillation of mice on the proportion of Treg ($CD4^+CD25^{high}FoxP3^+$) cells. Compared to the control group exposed to PBS, the proportion of Treg cells remained unchanged in spleen isolated from VGVAPG-treated mice (Fig. 5*A*). The lack of VGVAPG effects on the proportion of spleen Treg cells was also confirmed in lung and mLN (Fig. 5*B*). Similarly, the proportion of Treg cells among the cells isolated from lung, mLN and spleen of PPE-treated mice was not modified compared to control group (Fig. 5*B*).

Elastin peptides promote a Th-1/Th-17 and Tc-1 response in splenic T lymphocytes ex vivo. We next wondered whether an *ex vivo* interaction between EP and S-gal expressed on the surface of Th-1, Th-17 and Tc-1 pre-oriented T lymphocytes isolated from VGVAPG-exposed mice, may influence their cytokine expression. We first sorted $CD4^+$ and $CD8^+$ T cells from spleen of VGVAPG-treated mice and cultured them only with VGVAPG or elastin peptide mixture (EPM). Absence of significant effects on the proportion of IFN-γ or IL-17a expressing T cells (data not shown) leads us to culture the two sorted T cell subsets with anti-CD3/CD28 coated beads, in the absence (negative control, CT) or in the presence of VGVAPG or EPM. Compared to CT, addition of VGVAPG or EPM to stimulation media leads to a significant increase in the proportion of IFN-γ and IL-17a-expressing $CD4^+$ splenic T cells (Fig. 6*A*). This result was associated with a concomitant rise of activated $CD4^+$T-bet^+ and $CD4^+ROR\gamma t^+$ cells (Fig. 6*B*). Similar results were obtained with $CD4^+$ splenic T cells isolated from mice that received either PPE (Fig. 6*C* and 6*D*) or PBS (Fig. 6*E* and 6*F*). The presence of VGVAPG or EPM during $CD8^+$ splenic T cells stimulation also increased the

proportion of IFN-γ expressing cells isolated from VGVAPG-treated mice (Fig. 7*A*) as well as PPE- and PBS-instilled mice (Fig. 7*C* and 7*E*). These observations were confirmed by T-bet expression profile analysis of the same stimulated $CD8^+$ T cells (Fig. 7*B*, 7*D* and 7*F*).

S-gal-specific antagonist peptide inhibits local Th-1/Th-17 and Tc-1 response in VGVAPG-treated mice and PPE-treated mice. To further investigate whether Th-1/Th-17 and Tc-1 related cytokine response in VGVAPG-treated mice was linked to EP interaction with S-gal, we co-instilled mice with VGVAPG and the analogous peptide PGAIP that antagonizes the elastin peptide/elastin receptor interactions. This peptide was identified in a previous study as an inactive C-terminal glycine deleted-elastin peptide that retains its binding-activity to elastin receptor and inhibits the *in vitro* and *in vivo* activities of emphysema-inducing VGVAPG (34). We also co-instilled mice group with PPE and the antagonist peptide PGAIP to confirm our blocking strategy. In lung, mLN and spleen of mice co-treated with VGVAPG and PGAIP, the proportion of anti-CD3/CD28-activated $CD4^+$ T cell was highly reduced compared to mice in which VGVAPG was used alone, and reached values comparable to those obtained in PBS-instilled mice and PGAIP-instilled mice (Fig. 8*A*, 8*C and* 8*E*). As expected, this negative shift was correlated with a significant decreased expression of the transcription factors T-bet and RORγt analyzed in the same experimental conditions (Fig. 8*B*, 8*D and* 8*F*). Regarding $CD8^+$ T cell in lung, mLN and spleen, as a consequence of PGAIP efficiency, expression of IFN-γ and T-bet transcription factor was also significantly lowered in PGAIP/VGVAPG co-treated mice as revealed by values equivalent to those of PBS-treated mice and PGAIP-instilled mice (Fig. 9). The same blocking effect of PGAIP was observed in PPE/PGAIP co-instilled mice on $CD4^+$ and $CD8^+$ T cells cytokines and transcription factors expression (Fig. 8 and Fig. 9).

DISCUSSION

Several pieces of evidence are pointing towards an important role of T lymphocytes and elastin-derived peptides (EP) in the development and progression of pulmonary emphysema. The present study was designed to evaluate the effects of EP interaction with the elastin receptor S-gal on the Th and Tc responses during murine emphysema.

Induction of emphysema-like phenotype in mice following administration of EP, i.e. the VGVAPG peptide, is associated with an increased IFN-γ and IL-17a expression by lung and mLN-infiltrating $CD4^+$ T cells. These data are consistent with increase of T cell content in the BALF of VGVAPG-exposed mice. Interestingly, it has been reported that the lung T cell response is initially localized in the mLN and spreads systemically after 4 days (21). Consistent with these data, we observed a Th-1 (IFN-γ) and Th-17 (IL-17a) differentiation in $CD4^+$ splenic T cells of VGVAPG-treated mice. Moreover, we found that intrapulmonary and systemic Th cell phenotypes are driven by T-bet and RORγt transcription factors, confirming their polarization (20, 39). An increase of IFN-γ and T-bet transcription factor was also observed in activated $CD8^+$ T cells isolated from lung, mLN and spleen of VGVAPG-treated mice, supporting recent data that showed a pro-inflammatory phenotype among Tc cells isolated from lung of cigarette smoke (CS)-exposed mice (10). Furthermore, we demonstrated in this study that mice exposed to PPE, a well described emphysema mice model also exhibited a Th-1/Th-17 and Tc-1 orientation of T cells, suggesting that various inducers can promote such a pro-inflammatory T response during emphysematous process. This analysis is supported by previous human and mice reports that described *i/* the coexistence of a Th-1 and Th-17-biased $CD4^+$ T cell response in the pulmonary airspaces of chronic CS-exposed mice (15) and in the emphysematous lung of COPD patients (8, 14), and *ii/* an emphysema-associated Tc-1 response in CS-mice models (25) and COPD patients (7).

T helper response is known to be regulated by appropriated Treg counterbalance effects (42). In COPD, this condition remains to be clearly elucidated. In our experimental conditions, we found that Treg cell proportion is unchanged in VGVAPG- or PPE-treated mice compared to control mice. Similar results were obtained in an acute murine model of CS-induced emphysema (10), whereas a chronic CS-exposure of mice induces an increase in pulmonary Treg number (6). Such discrepancy is also noticed in COPD patients' studies (2, 22, 29, 38). These contradictory results could be easily explained by the differences in their experimental designs. A complete multicolor-phenotypic and functional exploration of Treg in COPD patients may resolve this controversy.

We have previously established a correlation between a type-1 profile and S-gal expression on EP treated human lymphocytes (5). In addition, we recently demonstrated in mice that VGVAPG-induced emphysema was associated with elastin breakdown, and that deleterious effects of soluble EP on lungs could be antagonized by analogous elastin peptides (34). Moreover, EP specific monoclonal antibodies treatment was previously described, by others, to suppress macrophages accumulation and airspace pathology development in PPE-recipient mice (19). In the present study, we demonstrated that EP- and PPE-instilled mice display a Th-1/Th-17 and Tc-1 cytokine expression pattern in lung, mLN and spleen. We therefore postulated that EP exert a central role in the development of a Th/Tc response during emphysema in mice whatever the etiologic inducer used.

In support to this hypothesis, the present study showed that the proportion of splenic T cells expressing type-1 or type-17 cytokines following VGVAPG or PPE instillation in mice was maximized after an *ex vivo* activation either by an elastin peptide mixture or the VGVAPG peptide. Given that this increase was also seen from the spleen of mice instilled with PBS, we can conclude that the results obtained from the spleens of VGVAPG- or PPE-instilled mice are not the consequence of the expansion of EP-specific T cell clones generated

following instillation but the consequence of EP/S-gal interaction independently of any EP presentation to the TCR. In line with these results, we previously demonstrated in human peripheral blood lymphocytes that S-gal occupancy by EP leads to the activation of extracellular signal-regulated kinase 1/2 (ERK1/2) and activation protein-1 (AP-1) DNAbinding, key actors in the coordination of IFN-γ transcription (5).

Based on the postulate of a correlation between type-1/ type-17 cytokine production and EP/S-gal interactions on T cells, we envisaged using an elastin receptor antagonist to prove the involvement of S-gal in pulmonary T lymphocytes response. In a previous report, we described that the PGAIP peptide antagonizes the VGVAPG/S-gal interactions and abolish in mice not only the EP-dependent pulmonary emphysema but also The PPE-induced emphysema (34). We demonstrated that the PGAIP peptide protects mice from the VGVAPG- and the PPE-dependent inflammatory cell infiltration in pulmonary tissue, MMP and desmosine accumulation in BALF, and parenchymal degradation. In this study, the S-gal-specific antagonist PGAIP peptide injected into murine lungs simultaneously with the VGVAPG peptide or PPE succeeded to impair the activity of etiologic inductor on Th-1/Th-17 and Tc-1 response. This result confirms the implication of S-gal receptor in T lymphocyte response during emphysema both when EP were directly administered or when they were induced par PPE biological effects. This regulation is also consistent with previously reported effects of PGAIP peptide on the protection of mice from the EP- or PPE-induced emphysema (34).

Integrated in the pathophysiological mechanisms of COPD, our results highlight an additional EP deleterious role in the generation and maintenance of the persistent inflammation observed in COPD patients. These results demonstrate that EP, whose genesis is perpetuated by induction of a self-amplification loop of inflammatory cells recruitment and proteases production, orchestrate an emphysema-associated inflammatory process through the

combined production of IFN-γ and IL-17, two cytokines linked to lung destruction (37) (Fig. 10). Via the production of IFN-γ, EP favour emphysema development, dysregulation of the pulmonary proteases/anti-proteases balance (43) and major the Th-1 pro-inflammatory response (33). Through the production of both IFN-γ and IL-17, EP enhance the recruitment of neutrophils into the airways (28).

Taken as a whole, our data confirm the critical role of Th-1, Th-17 and Tc-1 cells in the development of emphysema and highlight the effects of the EP/S-gal interactions on T cell orientation towards a pro-inflammatory profile. Our findings also provide evidence that this orientation might be controlled by S-gal specific antagonist peptides making them potential complementary therapeutic support to prevent the progression of the inflammatory process during emphysema. Studies are in progress, to investigate the potentiality of PGAIP to control a pre-existing inflammation induced by various emphysema inducers.

ACKNOWLEDGEMENTS

This work was supported by the University of Reims Champagne-Ardenne and by a grant-in-Aid "Contrat de Plan Etat-Région".

GRANTS

A.Meghraoui-Kheddar received a Grant for doctoral training from the French Ministry of Higher Education and Research and from the University of Reims Champagne-Ardenne.

DISCLOSURES

No conflicts of interest, financial or otherwise, are declared by the authors

REFERENCES

1. Baranek T, Debret R, Antonicelli F, Lamkhioued B, Belaaouaj A, Hornebeck W, Bernard P, Guenounou M, and Le Naour R. Elastin receptor (spliced galactosidase) occupancy by elastin peptides counteracts proinflammatory cytokine expression in lipopolysaccharide-stimulated human monocytes through NF-kappaB down-regulation. *J Immunol* 179: 6184-6192, 2007.

2. Barcelo B, Pons J, Ferrer JM, Sauleda J, Fuster A, and Agusti AG. Phenotypic characterisation of T-lymphocytes in COPD: abnormal CD4+CD25+ regulatory T-lymphocyte response to tobacco smoking. *Eur Respir J* 31: 555-562, 2008.

3. Barczyk A, Pierzchala W, Kon OM, Cosio B, Adcock IM, and Barnes PJ. Cytokine production by bronchoalveolar lavage T lymphocytes in chronic obstructive pulmonary disease. *J Allergy Clin Immunol* 117: 1484-1492, 2006.

4. Bhavani S, Tsai CL, Perusich S, Hesselbacher S, Coxson H, Pandit L, Corry DB, and Kheradmand F. Clinical and Immunological Factors in Emphysema Progression. Five-Year Prospective Longitudinal Exacerbation Study of Chronic Obstructive Pulmonary Disease (LES-COPD). *Am J Respir Crit Care Med* 192: 1171-1178, 2015.

5. Debret R, Antonicelli F, Theill A, Hornebeck W, Bernard P, Guenounou M, and Le Naour R. Elastin-derived peptides induce a T-helper type 1 polarization of human blood lymphocytes. *Arterioscler Thromb Vasc Biol* 25: 1353-1358, 2005.

6. Demoor T, Bracke KR, Joos GF, and Brusselle GG. Increased T-regulatory cells in lungs and draining lymph nodes in a murine model of COPD. *Eur Respir J* 35: 688-689, 2010.

7. Di Stefano A, Caramori G, Capelli A, Gnemmi I, Ricciardolo FL, Oates T, Donner CF, Chung KF, Barnes PJ, and Adcock IM. STAT4 activation in smokers and patients with chronic obstructive pulmonary disease. *Eur Respir J* 24: 78-85, 2004.

8. Di Stefano A, Caramori G, Gnemmi I, Contoli M, Vicari C, Capelli A, Magno F, D'Anna SE, Zanini A, Brun P, Casolari P, Chung KF, Barnes PJ, Papi A, Adcock I, and Balbi B. T helper type 17-related cytokine expression is increased in the bronchial mucosa of stable chronic obstructive pulmonary disease patients. *Clin Exp Immunol* 157: 316-324, 2009.

9. Dupont A, Dury S, Gafa V, Lebargy F, Deslee G, Guenounou M, Antonicelli F, and Le Naour R. Impairment of neutrophil reactivity to elastin peptides in COPD. *Thorax* 68: 421-428, 2013.

10. Eppert BL, Wortham BW, Flury JL, and Borchers MT. Functional characterization of T cell populations in a mouse model of chronic obstructive pulmonary disease. *J Immunol* 190: 1331-1340, 2013.

11. Freeman CM, Stolberg VR, Crudgington S, Martinez FJ, Han MK, Chensue SW, Arenberg DA, Meldrum CA, McCloskey L, and Curtis JL. Human CD56+ cytotoxic lung lymphocytes kill autologous lung cells in chronic obstructive pulmonary disease. *PLoS One* 9: e103840, 2014.

12. Ghuysen-Itard AF, Robert L, and Jacob MP. [Effect of elastin peptides on cell proliferation]. *C R Acad Sci III* 315: 473-478, 1992.

13. Goldstein RA, and Starcher BC. Urinary excretion of elastin peptides containing desmosin after intratracheal injection of elastase in hamsters. *J Clin Invest* 61: 1286-1290, 1978.

14. Grumelli S, Corry DB, Song LZ, Song L, Green L, Huh J, Hacken J, Espada R, Bag R, Lewis DE, and Kheradmand F. An immune basis for lung parenchymal destruction in chronic obstructive pulmonary disease and emphysema. *PLoS Med* 1: e8, 2004.

15. Harrison OJ, Foley J, Bolognese BJ, Long E, 3rd, Podolin PL, and Walsh PT. Airway infiltration of CD4+ CCR6+ Th17 type cells associated with chronic cigarette smoke induced airspace enlargement. *Immunol Lett* 121: 13-21, 2008.

16. Hinek A. Nature and the multiple functions of the 67-kD elastin-/laminin binding protein. *Cell Adhes Commun* 2: 185-193, 1994.

17. Hodge G, Nairn J, Holmes M, Reynolds PN, and Hodge S. Increased intracellular T helper 1 proinflammatory cytokine production in peripheral blood, bronchoalveolar lavage and intraepithelial T cells of COPD subjects. *Clin Exp Immunol* 150: 22-29, 2007.

18. Hogg JC, Chu F, Utokaparch S, Woods R, Elliott WM, Buzatu L, Cherniack RM, Rogers RM, Sciurba FC, Coxson HO, and Pare PD. The nature of small-airway obstruction in chronic obstructive pulmonary disease. *N Engl J Med* 350: 2645-2653, 2004.

19. Houghton AM, Quintero PA, Perkins DL, Kobayashi DK, Kelley DG, Marconcini LA, Mecham RP, Senior RM, and Shapiro SD. Elastin fragments drive disease progression in a murine model of emphysema. *J Clin Invest* 116: 753-759, 2006.

20. Ivanov, II, McKenzie BS, Zhou L, Tadokoro CE, Lepelley A, Lafaille JJ, Cua DJ, and Littman DR. The orphan nuclear receptor RORgammat directs the differentiation program of proinflammatory IL-17+ T helper cells. *Cell* 126: 1121-1133, 2006.

21. Lambrecht BN, Pauwels RA, and Fazekas De St Groth B. Induction of rapid T cell activation, division, and recirculation by intratracheal injection of dendritic cells in a TCR transgenic model. *J Immunol* 164: 2937-2946, 2000.

22. Lee SH, Goswami S, Grudo A, Song LZ, Bandi V, Goodnight-White S, Green L, Hacken-Bitar J, Huh J, Bakaeen F, Coxson HO, Cogswell S, Storness-Bliss C, Corry DB, and Kheradmand F. Antielastin autoimmunity in tobacco smoking-induced emphysema. *Nat Med* 13: 567-569, 2007.

23. Lombard C, Arzel L, Bouchu D, Wallach J, and Saulnier J. Human leukocyte elastase hydrolysis of peptides derived from human elastin exon 24. *Biochimie* 88: 1915-1921, 2006.

24. Majori M, Corradi M, Caminati A, Cacciani G, Bertacco S, and Pesci A. Predominant TH1 cytokine pattern in peripheral blood from subjects with chronic obstructive pulmonary disease. *J Allergy Clin Immunol* 103: 458-462, 1999.

25. Motz GT, Eppert BL, Sun G, Wesselkamper SC, Linke MJ, Deka R, and Borchers MT. Persistence of lung CD8 T cell oligoclonal expansions upon smoking cessation in a mouse model of cigarette smoke-induced emphysema. *J Immunol* 181: 8036-8043, 2008.

26. Owen CA. Proteinases and oxidants as targets in the treatment of chronic obstructive pulmonary disease. *Proc Am Thorac Soc* 2: 373-385; discussion 394-375, 2005.

27. Owen CA. Roles for proteinases in the pathogenesis of chronic obstructive pulmonary disease. *Int J Chron Obstruct Pulmon Dis* 3: 253-268, 2008.

28. Prause O, Bozinovski S, Anderson GP, and Linden A. Increased matrix metalloproteinase-9 concentration and activity after stimulation with interleukin-17 in mouse airways. *Thorax* 59: 313-317, 2004.

29. Roos-Engstrand E, Ekstrand-Hammarstrom B, Pourazar J, Behndig AF, Bucht A, and Blomberg A. Influence of smoking cessation on airway T lymphocyte subsets in COPD. *COPD* 6: 112-120, 2009.

30. Saetta M, Di Stefano A, Turato G, Facchini FM, Corbino L, Mapp CE, Maestrelli P, Ciaccia A, and Fabbri LM. CD8+ T-lymphocytes in peripheral airways of smokers with chronic obstructive pulmonary disease. *Am J Respir Crit Care Med* 157: 822-826, 1998.

31. Schild K, Knobloch J, Yakin Y, Jungck D, Urban K, Muller K, and Koch A. IL-5 release of CD4+ non-effector lymphocytes is increased in COPD--modulating effects of moxifloxacin and dexamethasone. *Int Immunopharmacol* 11: 444-448, 2011.

32. Schriver EE, Davidson JM, Sutcliffe MC, Swindell BB, and Bernard GR. Comparison of elastin peptide concentrations in body fluids from healthy volunteers, smokers, and patients with chronic obstructive pulmonary disease. *Am Rev Respir Dis* 145: 762-766, 1992.

33. Schroder K, Hertzog PJ, Ravasi T, and Hume DA. Interferon-gamma: an overview of signals, mechanisms and functions. *J Leukoc Biol* 75: 163-189, 2004.

34. Sellami M, Meghraoui-Kheddar A, Terryn C, Fichel C, Bouland N, Diebold MD, Guenounou M, Hery-Huynh S, and Le Naour R. Induction and regulation of murine emphysema by elastin peptides. *Am J Physiol Lung Cell Mol Physiol* 310: L8-23, 2016.

35. Senior RM, Griffin GL, Mecham RP, Wrenn DS, Prasad KU, and Urry DW. Val-Gly-Val-Ala-Pro-Gly, a repeating peptide in elastin, is chemotactic for fibroblasts and monocytes. *J Cell Biol* 99: 870-874, 1984.

36. Shan M, Cheng HF, Song LZ, Roberts L, Green L, Hacken-Bitar J, Huh J, Bakaeen F, Coxson HO, Storness-Bliss C, Ramchandani M, Lee SH, Corry DB, and Kheradmand F. Lung myeloid dendritic cells coordinately induce TH1 and TH17 responses in human emphysema. *Sci Transl Med* 1: 4ra10, 2009.

37. Shan M, Yuan X, Song LZ, Roberts L, Zarinkamar N, Seryshev A, Zhang Y, Hilsenbeck S, Chang SH, Dong C, Corry DB, and Kheradmand F. Cigarette smoke induction of osteopontin (SPP1) mediates T(H)17 inflammation in human and experimental emphysema. *Sci Transl Med* 4: 117ra119, 2012.

38. Smyth LJ, Starkey C, Vestbo J, and Singh D. CD4-regulatory cells in COPD patients. *Chest* 132: 156-163, 2007.

39. Szabo SJ, Sullivan BM, Stemmann C, Satoskar AR, Sleckman BP, and Glimcher LH. Distinct effects of T-bet in TH1 lineage commitment and IFN-gamma production in CD4 and CD8 T cells. *Science* 295: 338-342, 2002.

40. Urbanowicz RA, Lamb JR, Todd I, Corne JM, and Fairclough LC. Enhanced effector function of cytotoxic cells in the induced sputum of COPD patients. *Respir Res* 11: 76, 2010.

41. Vestbo J, Hurd SS, Agusti AG, Jones PW, Vogelmeier C, Anzueto A, Barnes PJ, Fabbri LM, Martinez FJ, Nishimura M, Stockley RA, Sin DD, and Rodriguez-Roisin R. Global strategy for the diagnosis, management, and prevention of chronic obstructive pulmonary disease: GOLD executive summary. *Am J Respir Crit Care Med* 187: 347-365, 2013.

42. Wang H, Peng W, Weng Y, Ying H, Li H, Xia D, and Yu W. Imbalance of Th17/Treg cells in mice with chronic cigarette smoke exposure. *Int Immunopharmacol* 14: 504-512, 2012.

43. Wang Z, Zheng T, Zhu Z, Homer RJ, Riese RJ, Chapman HA, Jr., Shapiro SD, and Elias JA. Interferon gamma induction of pulmonary emphysema in the adult murine lung. *J Exp Med* 192: 1587-1600, 2000.

44. Xu C, Hesselbacher S, Tsai CL, Shan M, Spitz M, Scheurer M, Roberts L, Perusich S, Zarinkamar N, Coxson H, Krowchuk N, Corry DB, and Kheradmand F. Autoreactive T Cells in Human Smokers is Predictive of Clinical Outcome. *Front Immunol* 3: 267, 2012.

FIGURE CAPTIONS

Fig. 1. Increased number of T lymphocyte subpopulations in the cell infiltrate observed during VGVAPG-dependent emphysema. *A:* flow cytometry analysis and specific cell count in the BALF of mice 2 days-exposed to PBS, PPE (7.4 µg/ml) or VGVAPG (10 µg/ml). *B*: auto-fluorescent analysis of elastin and collagen fibers organization in the lungs of mice at day-21 (63x). *C*: ratio index of the elastin-to-collagen structures measured from a 3D mapping of lung extracellular matrix components performed at day-21. *D*: morphological representation of Hematoxylin Phloxin Safran-stained lung sections obtained from mice at day-21 (100x). *E*: mean linear intercept measured from Hematoxylin Phloxin Safran-stained lung sections performed at day-21. *F*: desmosine concentrations measured in BAL fluids and *sera* collected from mice at day-21 following PBS, PPE or VGVAPG instillation. In these experiments, n = 7 to 16 mice per group. Photomicropraphs are representative of three separate experiments and data represent mean of values from four separate experiments ± SEM. $^{***}p< 0.001$, $^{**}p< 0.01$, $^{*}p< 0.05$.

Fig. 2. Exposure of mice to VGVAPG increases the proportion of $CD4^+$ T cells expressing IFN-γ and IL-17a in lung, mLN and spleen. Flow cytometry analysis of intracellular cytokine expression (IFN-γ, IL-17a and IL-4) (*A*) and transcription factor expression (T-bet, RORγt and GATA3) (*B*) performed after anti-CD3/CD28 stimulation of $CD45^+$ T cells from lung, mLN and spleen of mice 21 days-exposed to PBS, PPE or VGVAPG. Values are expressed as percentage of activated $CD4^+CD25^+$ T cells expressing each cytokine or transcription factor. In these experiments, n = 7 to 15 mice per group and data represent mean of values from four separate experiments ± SEM. $^{***}p< 0.001$, $^{**}p< 0.01$, $^{*}p< 0.05$.

Fig. 3. Exposure of mice to VGVAPG increases the proportion of $CD8^+$ T cells expressing IFN-γ in lung, mLN and spleen. Flow cytometry analysis of intracellular cytokine expression (IFN-γ, IL-17a and IL-4) (*A*) and transcription factor expression (T-bet, RORγt and GATA3)

(*B*) performed after anti-CD3/CD28 stimulation of $CD45^+$ T cells from lung, mLN and spleen of mice 21-days exposed to PBS, PPE or VGVAPG. Values are expressed as percentage of activated $CD8^+CD25^+$ T cells expressing each cytokine or transcription factor. In these experiments, n = 5 to 12 mice per group and data represent mean of values from three separate experiments ± SEM. $^{***}p< 0.001$, $^{**}p< 0.01$, $^{*}p< 0.05$.

Fig. 4. Exposure of mice to VGVAPG induces IFN-γ production by both $CD4^+$ and $CD8^+$ splenic T cells and IL-17a production by $CD4^+$ T cells. Quantification of IFN-γ, IL17-a and IL-4 production in cell culture supernatants of anti-CD3/CD28-stimulated $CD4^+$ (*A*) or $CD8^+$ (*B*) splenic T cells performed by Cytometric Bead Array Analysis. In these experiments, n = 9 to 12 mice per group and data represent mean of values from three-four separate experiments ± SEM. $^{***}p< 0.001$, $^{**}p< 0.01$, $^{*}p< 0.05$.

Fig. 5. Treg cell proportion is not altered in lung, mLN and spleen of mice exposed to VGVAPG. (*A*) Flow cytometry analysis of CD25 and FoxP3 transcription factor co-expression after anti-CD3/CD28 activation of $CD4^+$ T cells isolated from the spleen of mice 21 days-exposed to PBS, PPE or VGVAPG. Data are representative of three independent experiments. (*B*) Percentage of $CD4^+CD25^{high}$ T cells expressing FoxP3 in the lung, mLN and spleen of mice 21 days-exposed to PBS, PPE or VGVAPG. In these experiments, n = 4 to 7 mice per group and data represent mean of values from two separate experiments ± SEM.

Fig. 6. EP potentiate IFN-γ and IL-17a-producing $CD4^+$ splenic T cells *ex vivo*. $CD4^+$ T cells sorted from the spleens of VGVAPG-, PPE- or PBS-treated mice were cultured with anti-CD3/CD28 beads in absence (CT) or presence of either elastin peptide mixture (EPM) or VGVAPG peptide. Intracellular IFN-γ and IL-17a expression (*A*, *C*, and *E*) and T-bet and RORγt expression (*B*, *D*, and *F*) were analyzed by flow cytometry. Values are expressed as percentage of activated $CD4^+CD25^+$ splenic T cells expressing each cytokine or transcription

factor. In these experiments, n = 6 to 15 mice pooled per group and data represent mean of values from four separate experiments ± SEM. $^{***}p< 0.001$, $^{**}p< 0.01$, $^{*}p< 0.05$.

Fig. 7. EP potentiate IFN-γ-producing $CD8^+$ splenic T cells *ex vivo*. $CD8^+$ T cells sorted from the spleens of VGVAPG-, PPE- or PBS-treated mice were cultured with anti-CD3/CD28 beads in absence (CT) or presence of either elastin peptide mixture (EPM) or VGVAPG peptide. Intracellular IFN-γ expression (*A*, *C*, and *E*) and T-bet expression (*B*, *D*, and *F*) were analyzed by flow cytometry. Values are expressed as percentage of activated $CD8^+CD25^+$ splenic T cells expressing each marker. In all experiments, n = 6 to 10 mice pooled per group and data represent mean of values from three separate experiments ± SEM. $^{**}p< 0.01$, $^{*}p< 0.05$.

Fig. 8. S-gal specific antagonist peptide PGAIP inhibits VGVAPG and PPE effects on Th-1 and Th-17 response in lung, mLN and spleen. Flow cytometry analysis of IFN-γ and IL-17a expression (*A*, *C*, and *E*) and T-bet and RORγt expression (*B*, *D*, and *F*) performed after anti-CD3/CD28 stimulation of $CD4^+$ T cells from lung, mLN and spleen of mice 21-days exposed to PBS, PPE, VGVAPG (VG), PGAIP (PG) or a mixture containing PPE and the PGAIP peptide (PPE+PG) or the VGVAPG and the PGAIP peptides (VG+PG). In these experiments, n = 7 to 17 mice per group and data represent mean of values from at least three separate experiments ± SEM. $^{***}p< 0.001$, $^{**}p< 0.01$, $^{*}p< 0.05$.

Fig. 9. S-gal specific antagonist peptide PGAIP inhibits VGVAPG and PPE effects on Tc-1 response in lung mLN and spleen. Flow cytometry analysis of IFNγ- expression (*A*, *C*, and *E*) and T-bet expression (*B*, *D*, and *F*) performed after anti-CD3/CD28 stimulation of $CD8^+$ T cells from lung, mLN and spleen of mice 21-days exposed to PBS, PPE, VGVAPG (VG), PGAIP (PG) or a mixture containing PPE and the PGAIP peptide (PPE+PG) or the VGVAPG and the PGAIP peptides (VG+PG). In these experiments, n = 7 to 17 mice per group and data

represent mean of values from three separate experiments ± SEM. $^{***}p< 0.001$, $^{**}p< 0.01$, $^{*}p< 0.05$.

Fig. 10. Key role of EP/S-gal interaction ~~in~~ the emphysema-associated inflammatory process. EP genesis perpetuated by a self-amplification loop of inflammatory cells recruitment (neutrophils and macrophages) and proteases release (neutrophil elastase, MMP-9 and MMP-12) is a key event to promote the combined production of IFNγ and IL-17 which orchestrate the inflammatory process associated with emphysema. EP effects are mediated via their interaction with the elastin receptor S-gal expressed on T cells and that can be controlled by S-gal specific antagonist peptides.

Figure 1

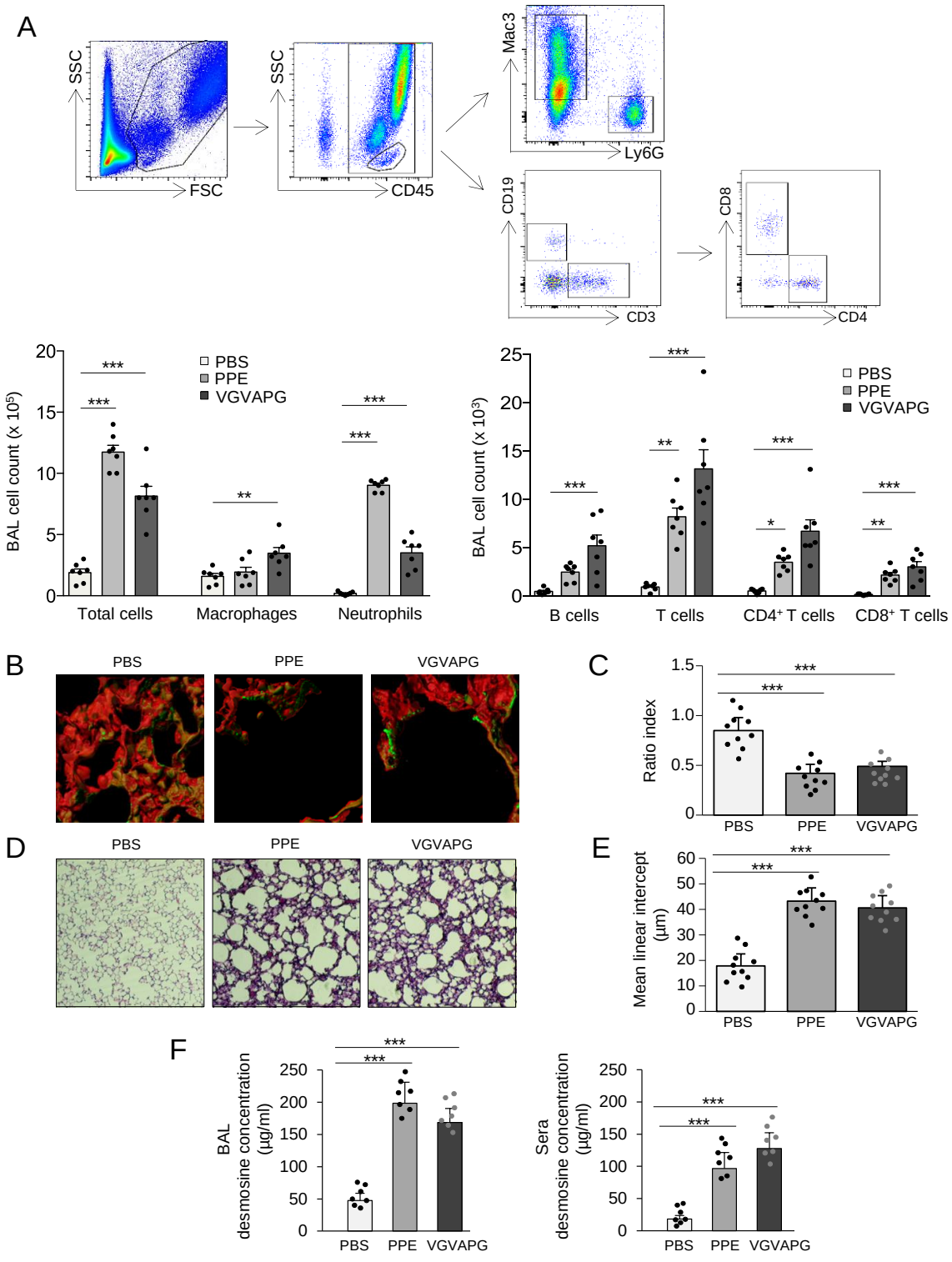
A
SSC
FSC
SSC
CD45
Mac3
Ly6G
CD19
CD3
CD8
CD4
BAL cell count (x 10⁵)
PBS
PPE
VGVAPG
Total cells
Macrophages
Neutrophils
BAL cell count (x 10³)
B cells
T cells
CD4⁺ T cells
CD8⁺ T cells
B
PBS
PPE
VGVAPG
C
Ratio index
D
E
Mean linear intercept (µm)
F
BAL desmosine concentration (µg/ml)
Sera desmosine concentration (µg/ml)

Figure 2

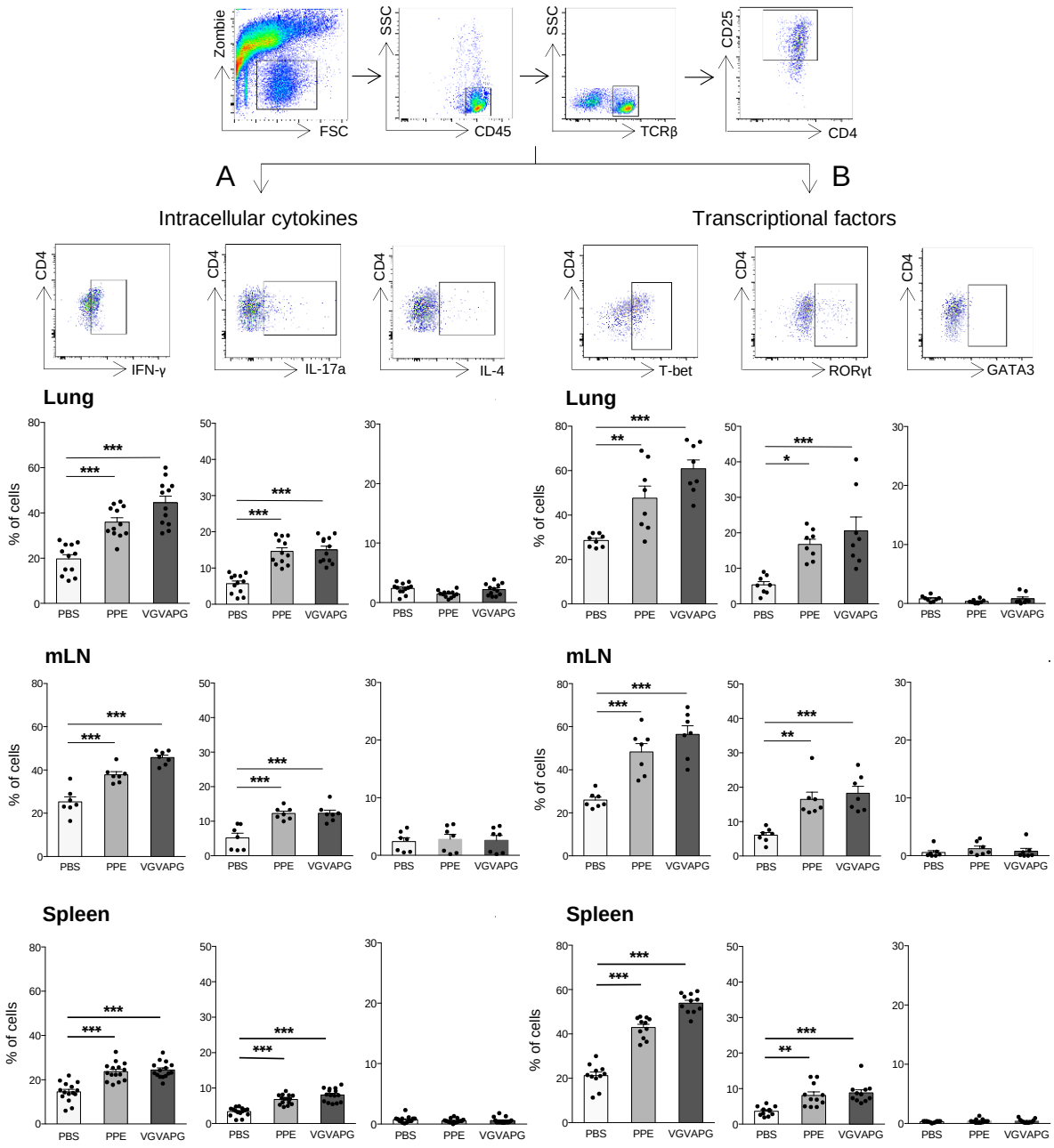
Zombie
FSC
SSC
CD45
SSC
TCRβ
CD25
CD4
A
B
Intracellular cytokines
Transcriptional factors
CD4
IFN-γ
IL-17a
IL-4
T-bet
RORγt
GATA3
Lung
mLN
Spleen
% of cells
PBS
PPE
VGVAPG

Figure 3

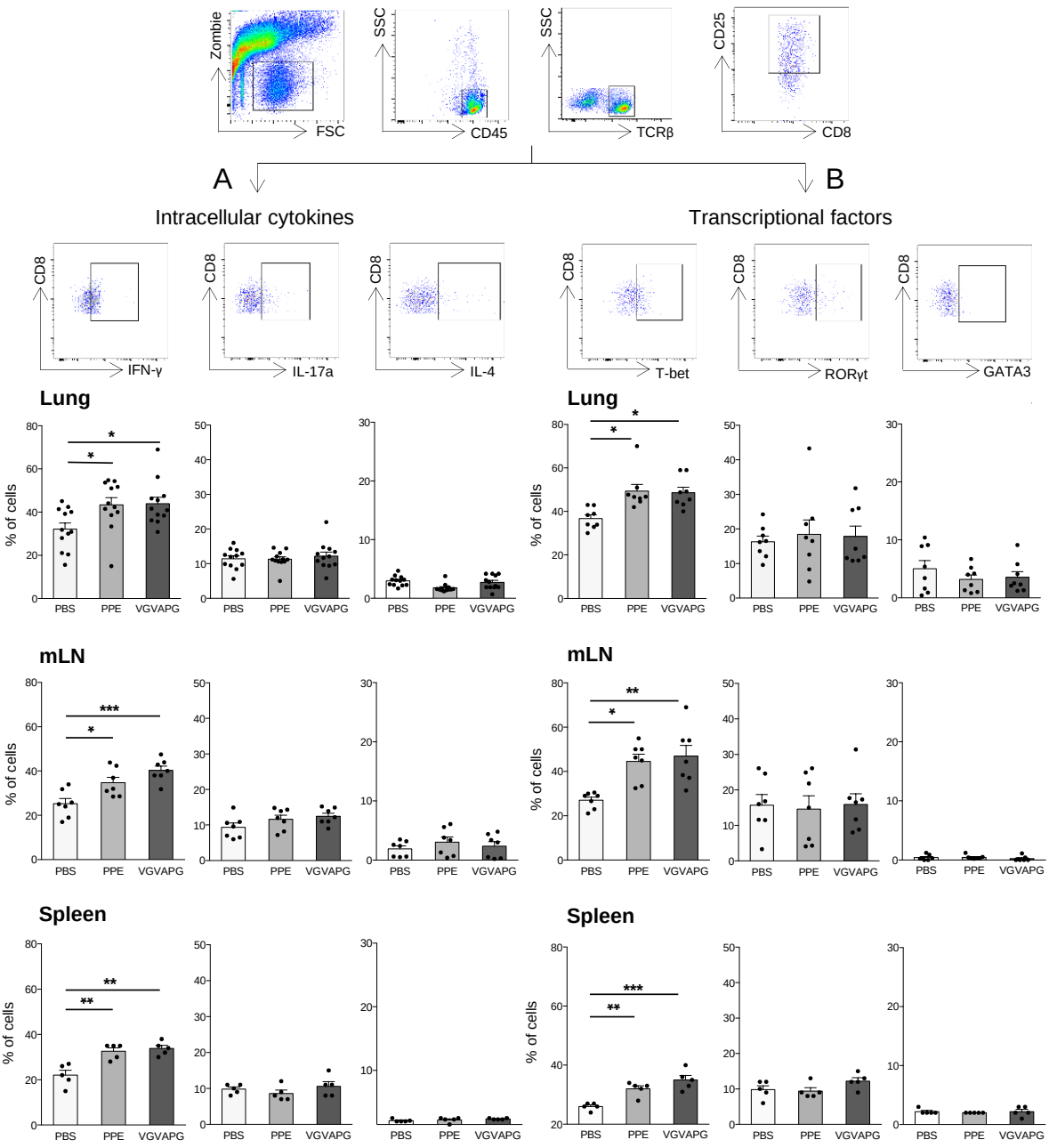
Zombie
FSC
SSC
CD45
SSC
TCRβ
CD25
CD8
A
B
Intracellular cytokines
Transcriptional factors
CD8
IFN-γ
IL-17a
IL-4
T-bet
RORγt
GATA3
Lung
mLN
Spleen
% of cells
PBS
PPE
VGVAPG

Figure 4

A : splenic CD4+ T cells

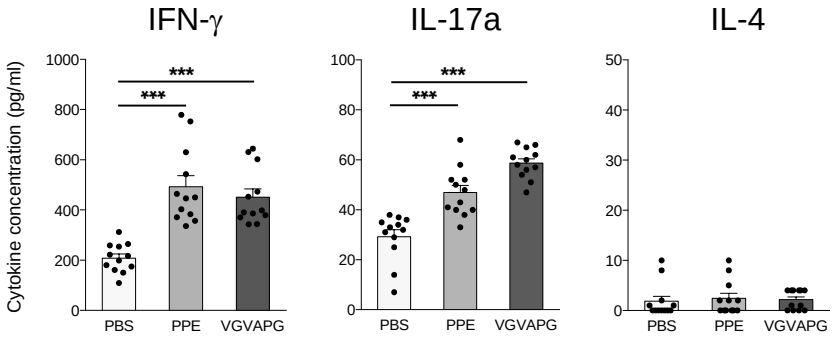

B : splenic CD8+ T cells

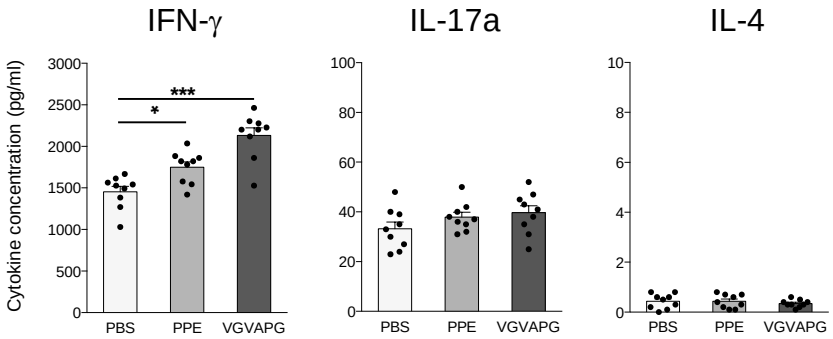

Figure 5

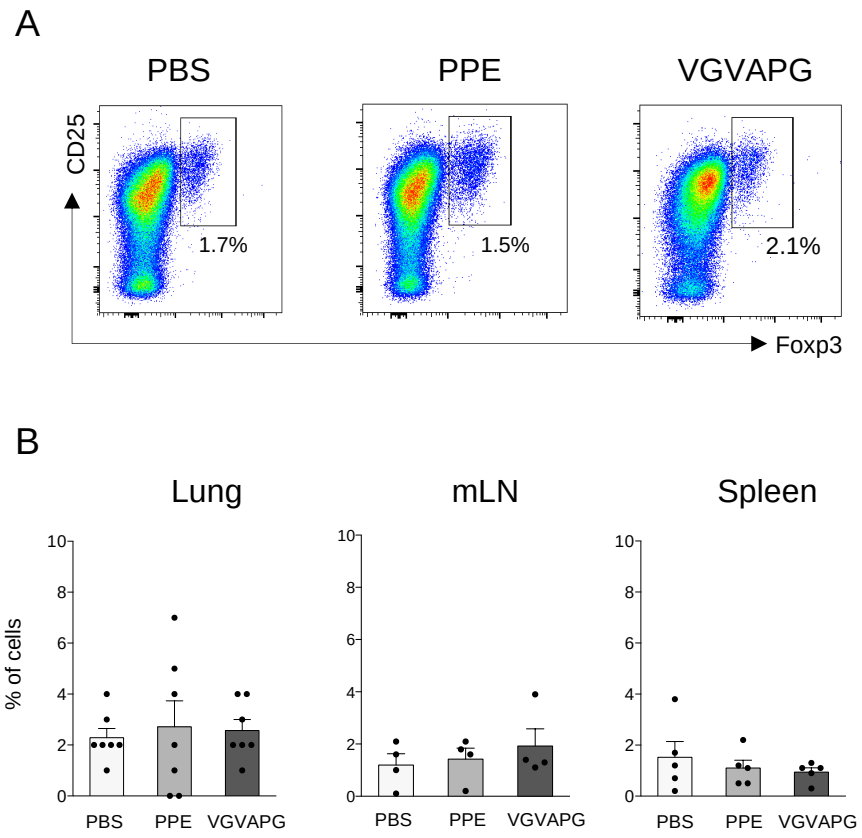
A
PBS
PPE
VGVAPG
CD25
1.7%
1.5%
2.1%
Foxp3
B
Lung
mLN
Spleen
% of cells
10
8
6
4
2
0
PBS
PPE
VGVAPG

Figure 6

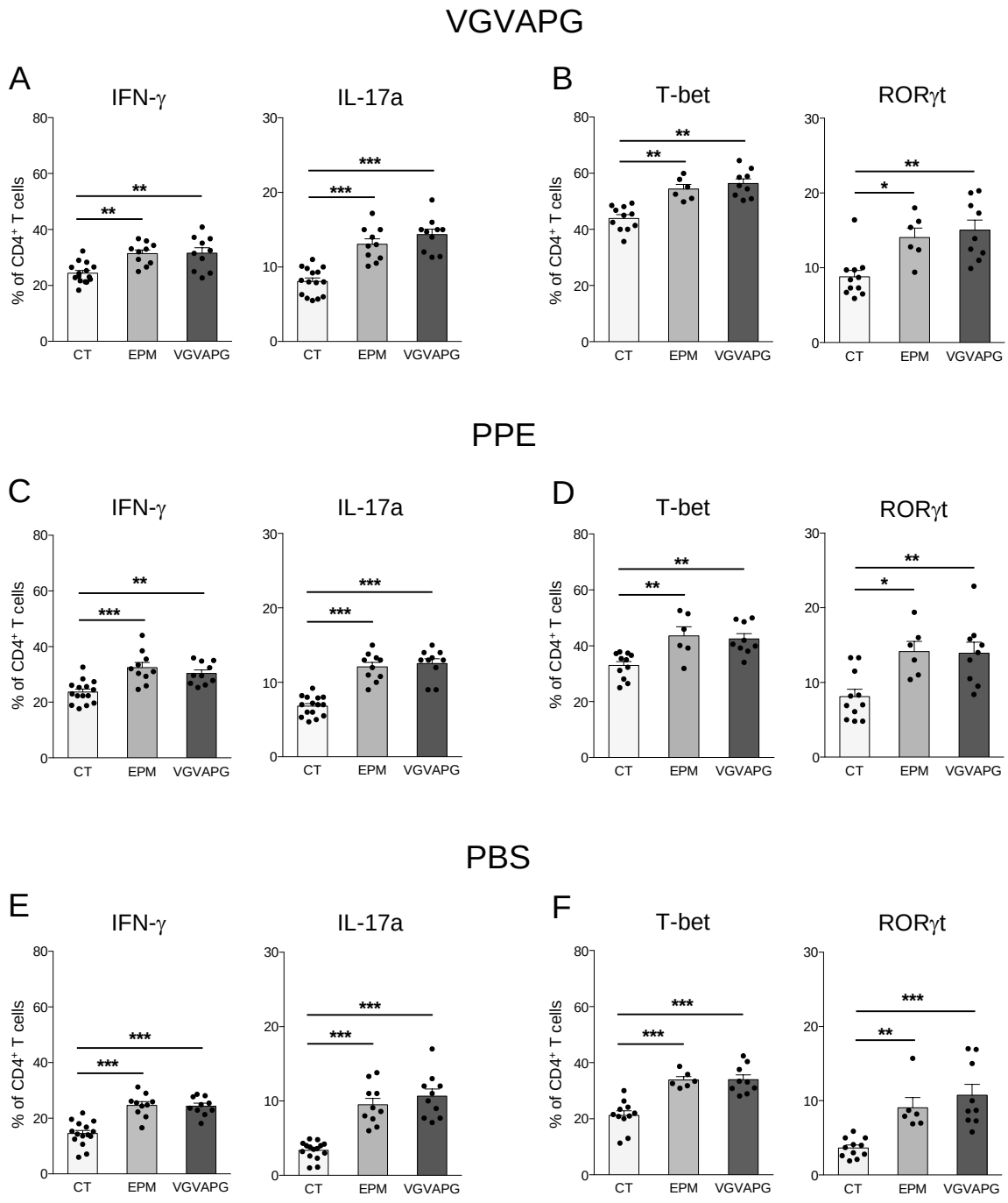
VGVAPG
A
IFN-γ
IL-17a
B
T-bet
RORγt
% of CD4⁺ T cells
CT
EPM
VGVAPG
PPE
C
IFN-γ
IL-17a
D
T-bet
RORγt
PBS
E
IFN-γ
IL-17a
F
T-bet
RORγt

Figure 7

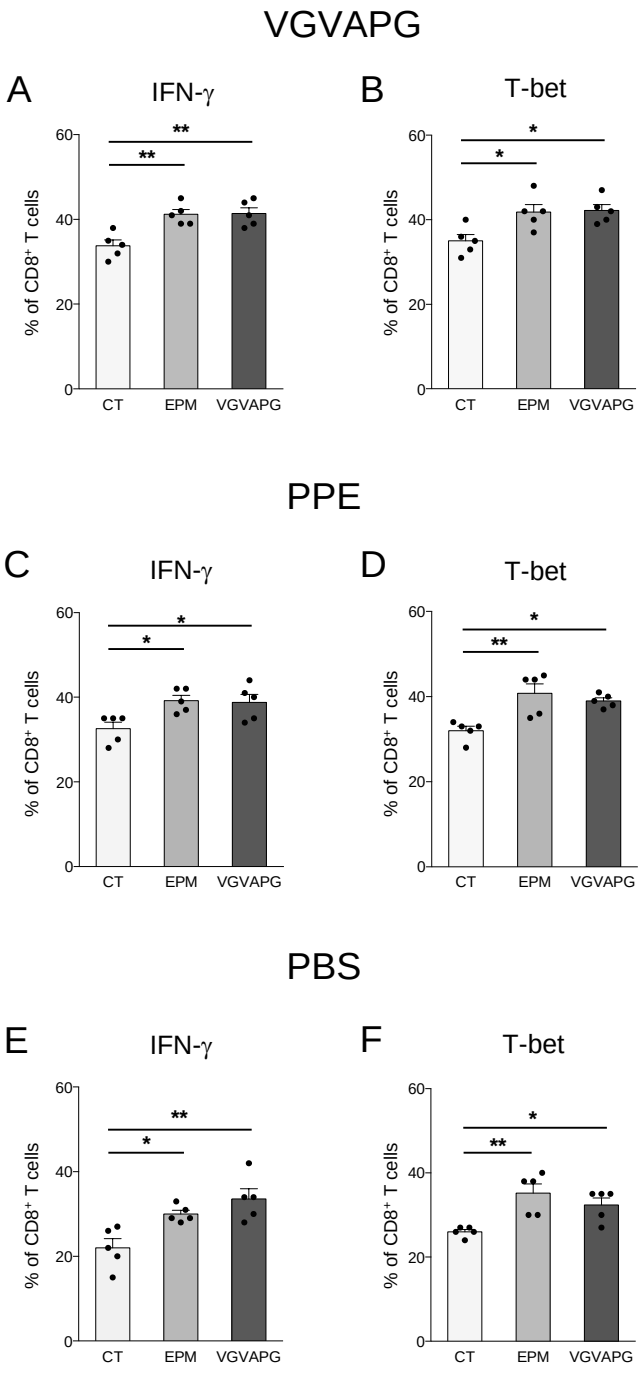
VGVAPG
A
IFN-γ
B
T-bet
% of CD8⁺ T cells
0
20
40
60
CT
EPM
VGVAPG
**
**
*
*
PPE
C
IFN-γ
D
T-bet
*
*
*
**
PBS
E
IFN-γ
F
T-bet
**
*
*
**

Figure 8

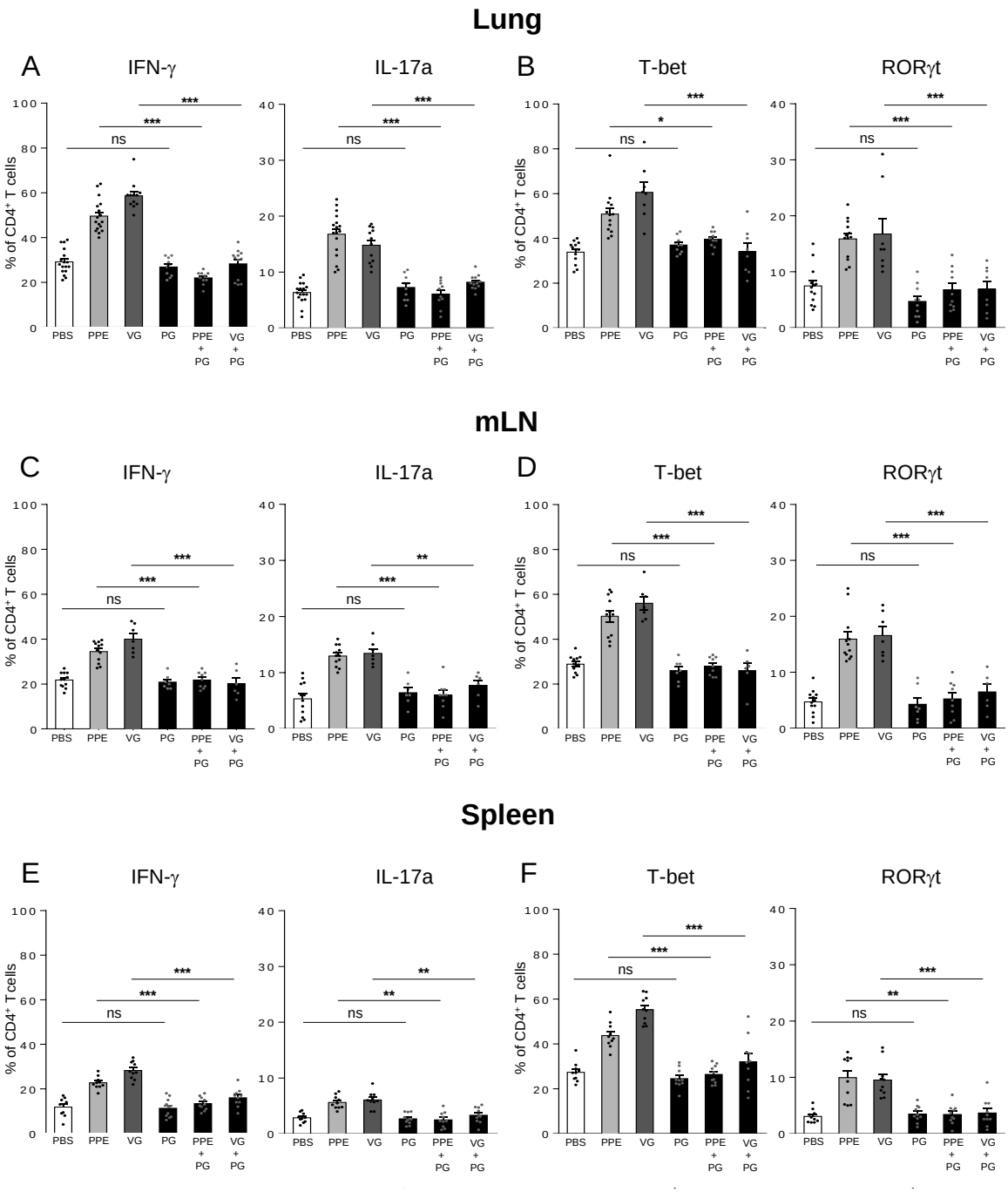
Lung
A
IFN-γ
IL-17a
B
T-bet
RORγt
% of CD4+ T cells
PBS
PPE
VG
PG
PPE + PG
VG + PG
ns
*
**
***
mLN
C
IFN-γ
IL-17a
D
T-bet
RORγt
Spleen
E
IFN-γ
IL-17a
F
T-bet
RORγt

Figure 9

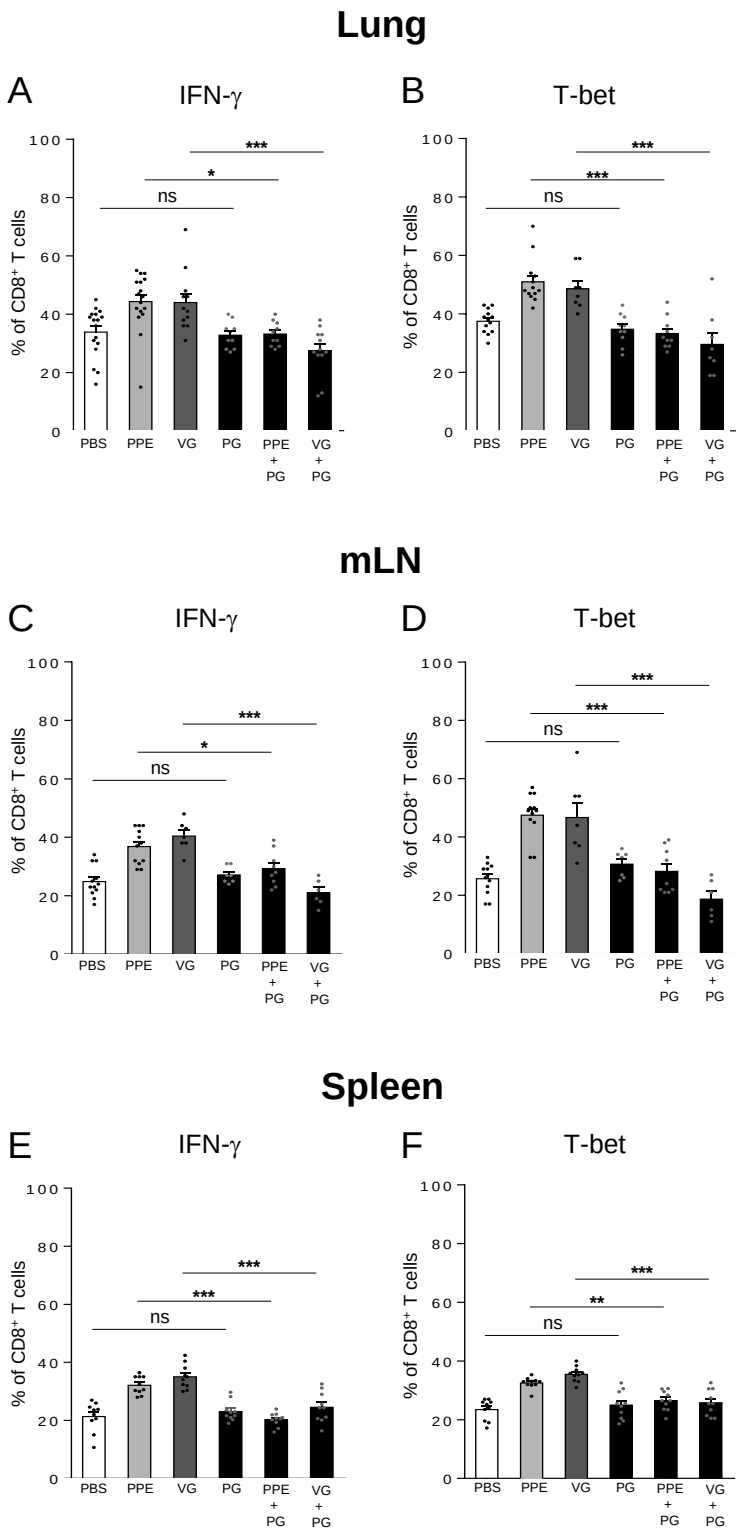
Lung
A
IFN-γ
B
T-bet
% of CD8+ T cells
ns
*
***
PBS
PPE
VG
PG
PPE + PG
VG + PG
mLN
C
IFN-γ
D
T-bet
Spleen
E
IFN-γ
F
T-bet
**

Figure 10

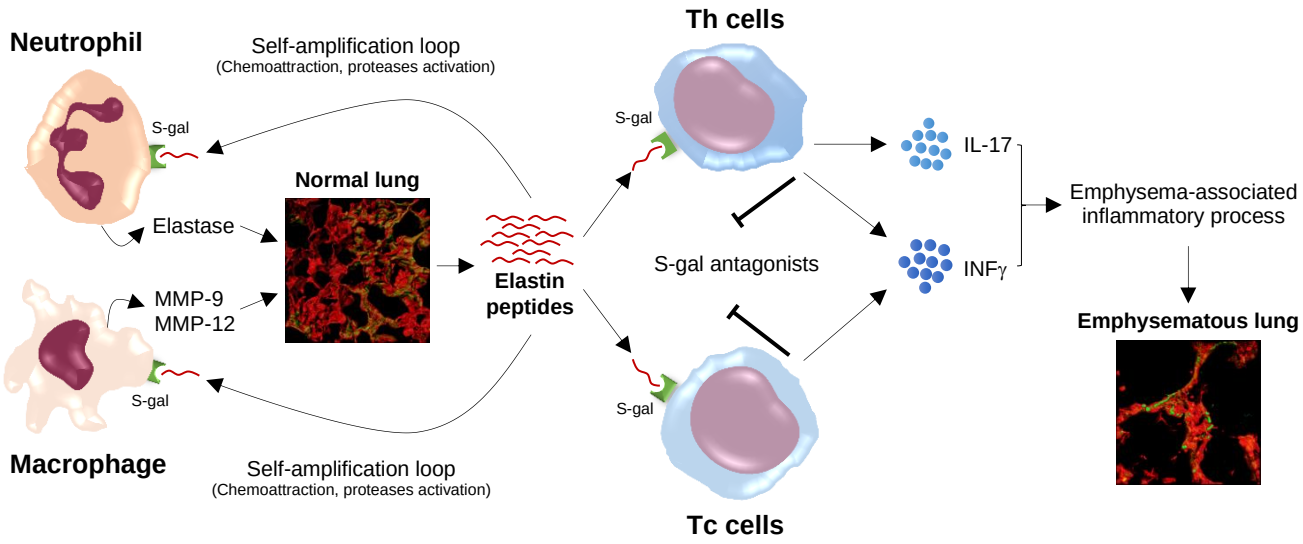
Neutrophil
Self-amplification loop
(Chemoattraction, proteases activation)
S-gal
Normal lung
Elastase
MMP-9
MMP-12
S-gal
Macrophage
Self-amplification loop
(Chemoattraction, proteases activation)
Elastin peptides
Th cells
S-gal
S-gal antagonists
S-gal
Tc cells
IL-17
INFγ
Emphysema-associated inflammatory process
Emphysematous lung